Syntheses and the Study of Strongly Hydrogen-Bonded Poly(vinylphenol-*b*-vinylpyridine) Diblock Copolymer through Anionic Polymerization

Shiao-Wei Kuo,* Pao-Hsiang Tung, and Feng-Chih Chang

Institute of Applied Chemistry, National Chiao Tung University, Hsinchu, Taiwan

Received July 27, 2006; Revised Manuscript Received November 2, 2006

ABSTRACT: A series of poly(vinylphenol-*b*-vinylpyridine) (PVPh-*b*-P4VP) block copolymers were prepared through anionic polymerizations of 4-*tert*-butoxystyrene with 4-vinylpyridine followed by subsequent selective hydrolysis of the 4-*tert*-butoxystyrene protective groups. Infrared spectrum analysis suggests that this block copolymer possesses strong hydrogen-bonding interaction between the hydroxyl group of PVPh and the pyridine group of P4VP. DSC analyses indicate that these PVPh-*b*-P4VP copolymers always have higher glass transition temperatures than the corresponding PVPh/P4VP miscible blends obtained from DMF solution. However, the thermal behavior of PVPh-*b*-P4VP diblock copolymer shows a similar T_g value with the PVPh/P4VP blend complex obtained from methanol solution at a 1:1 (PVPh:P4VP) molar ratio. We proposed that the polymer chain behavior of the PVPh/P4VP blend from DMF solution is separated coils. However, by increasing the hydrogen bonding for PVPh-*b*-P4VP diblock copolymer, a polymer complex aggregate is proposed, which is similar to the PVPh/P4VP blend complex from methanol solution. The spin−lattice relaxation time in the rotating frame ($T_{1\rho}^H$) based on solid-state NMR analysis is able to provide positive evidence that the polymer complex aggregate in the diblock copolymer has a shorter $T_{1\rho}^H$ value than the separated coils in the miscible blend.

Introduction

Miscible polymer blends have been of great interest to materials scientists because of their improved or modified properties over individual constituent polymers. A vast majority of the studies are aimed at enhancing the miscibility of polymer blends by incorporating local centers into the blend components that are capable of participating in strong hydrogen-bonding interactions.[1−3] It is well-known that the strength and extent of hydrogen bonding in copolymers or polymer blends depend on their respective affinities[4−6] between the hydrogen bond donors and acceptors.

Over the years, the polymer blend system of poly(vinylphenol)/poly(4-vinylpyridine) (PVPh/P4VP) has been classified as the strong hydrogen-bonding system, which has been widely discussed in previous studies.[7−11] PVPh has the strong proton donor group, and it has been reported that PVPh is miscible with many proton acceptor polymers such as polymethacrylate, polyether, and polyester.[12−17] P4VP has a similar structure to that of PVPh where the pyridine can also act as a proton acceptor group. Frechet[7] and Goh[8] have studied the miscibility and thermal behaviors of the PVPh/P4VP complex in low polar solvents such as methanol and ethanol to form a 1:1 (PVPh:P4VP) complex whose single T_g at 210 °C is significantly higher than each respective component of the blend (155 and 138 °C). This result can be attributed to the existence of strong hydrogen-bonding interactions between these two polymers to form thermally reversible cross-linking and thus significantly reduces the mobility of individual chains in this miscible polymer complex. In addition, the solvent medium plays an important role to affect or control the type of complex formation.[18] For example, the PVPh/poly(*N*,*N*-dimethylacrylamide) (PDMA) blend yields the complex precipitate in dioxane but causes no precipitation in DMF. Since solvent molecules can also participate in hydrogen-bonding interaction, therefore, they can compete with PDMA for hydroxyl groups in PVPh. The affinity of the hydrogen bond acceptor can be estimated comparing by the infrared frequency absorption difference ($\Delta\nu$) between the hydrogen-bonded hydroxyl and the free hydroxyl absorption of phenol (a model compound for PVPh). The dioxane is a relatively weaker hydrogen bond acceptor ($\Delta\nu = 235$ cm^{-1}) than the DMF ($\Delta\nu = 340$ cm^{-1}). Similarly, PVPh/P4VP blends also can form interpolymer complexes in methanol or ethanol. However, in DMF solution, such a strong hydrogen bond breaking solvent cannot form the interpolymer complex.[8,18] Furthermore, the T_g of the PVPh/P4VP complex obtained from ethanol solution is always higher than the miscible PVPh/P4VP blend from DMF solution casting.[8]

Scheme 1. Synthesis of Poly(vinylphenol-*b*-4-vinylpyridine) Diblock Copolymer by Anionic Polymerization

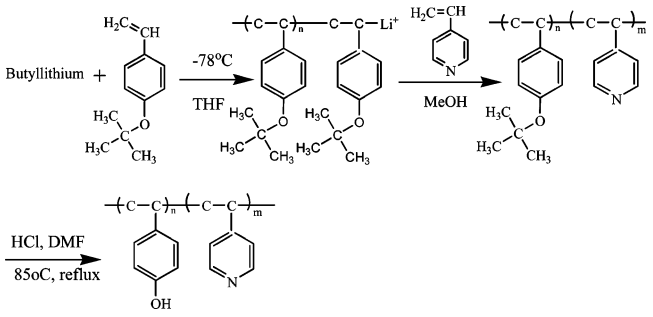

An interesting result from our previous study revealed that a random copolymer of PVPh-*co*-PMMA possesses a higher fraction of hydrogen-bonded carbonyl group and larger interassociation equilibrium constant than a block copolymer containing similar vinylphenol content because of the so-called intramolecular screening effect.[19] Painter and Coleman proposed[20] that "intramolecular screening effects" have a significant effect on the number of the hydrogen-bonded functional groups. The intramolecular screening effect is caused by an increase in

* To whom correspondence should be addressed: e-mail kuosw@mail.nctu.edu.tw; Tel 886-3-5131512; Fax 886-3-5131512.

10.1021/ma061713q CCC: $33.50
Published on Web 12/06/2006

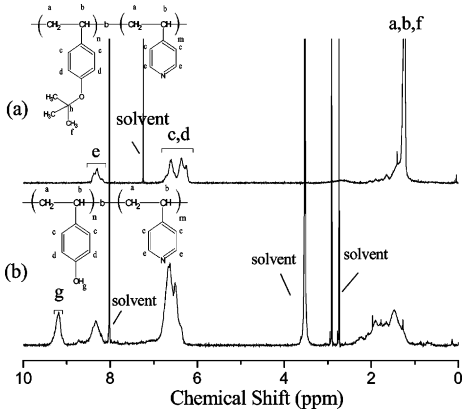

Figure 1. ^{1}H NMR spectra: (a) before hydrolysis, P*t*BOS-*b*-P4VP; (b) after hydrolysis, PVPh-*b*-P4VP.

the number of contacts by the same polymer chain due to polymer chain self-bending back, and the number of interassociation hydrogen-bondings per unit volume in the polymer blend will be less relative to the model compound. They used FT-IR spectroscopy to measure the fraction of hydrogen-bonded carbonyl groups present in miscible blends of poly(vinylphenol) (PVPh) with poly(ethyl methacrylate) (PEMA) as a function of composition and temperature. These results have been compared with analogous poly(ethyl methacrylate-*co*-vinylphenol) random copolymers and with low molecular weight model mixtures of 4-ethylphenol (EPH) and ethyl isobutylene (EIB).[21] They found a significant difference between polymer blend and random copolymer in the equilibrium fraction of intermolecular hydrogen-bonded carbonyl groups at identical composition and temperature.[21] However, the relationship of hydrogen-bonding strength and related polymer chain behavior between miscible polymer blend and miscible block copolymer is still not clearly understood on the basis of our knowledge.

We have previously reported that PPO-*b*-PS copolymers have higher glass transition temperatures than their corresponding PPO/PS blends.[22] In this study, we report the preparation of PVPh-*b*-P4VP diblock copolymers by combining protected group chemistry with anionic polymerization. The chemical structure, glass transition behavior, and specific interaction in these diblock copolymers were characterized by using ^{1}H NMR, DSC, FTIR, and ^{13}C solid-state NMR analyses.

Experimental Section

Materials. The 4-*tert*-butoxystyrene monomers (*t*BOS, Aldrich, 99%) and 4-vinylpyridine (Aldrich, 99%) were distilled from the finely ground CaH_2 before use. Tetrahydrofuran (THF) as the polymerization solvent for anionic polymerization was purified by distillation under argon from the red solution obtained by diphenylhexyllithium (produced by the reaction of 1,1-diphenylethylene and *n*-BuLi). *sec*-Butyllithium (Acros, 1.3 M in cyclohexane) was used as the initiator for anionic polymerization.

Syntheses of the Block Copolymers. Poly(4-*tert*-butoxystyrene-*b*-4-vinylpyridine) (P*t*BOS-*b*-P4VP) diblock copolymers were synthesized by sequential anionic polymerization of 4-*tert*-butoxystyrene and 4-vinylpyridine in tetrahydrofuran (THF) with *sec*-butyllithium as initiator. Lithium chloride (LiCl) was used to prevent side reaction and reduce the reactivity of the chain ends from 4-vinylpyridine polymerization.[23−27] Polymerizations were carried out under an inert atmosphere in a round-bottomed flask equipped with a rubber septum. Solvents, initiators, and monomers were transferred via a stainless capillary and syringe to the reactor. *sec*-Butyllithium was first added into the glass reactor containing the LiCl (was in 5-fold excess relative to the *sec*-butyllithium) in THF; a dark red color appeared. After the temperature was decreased to

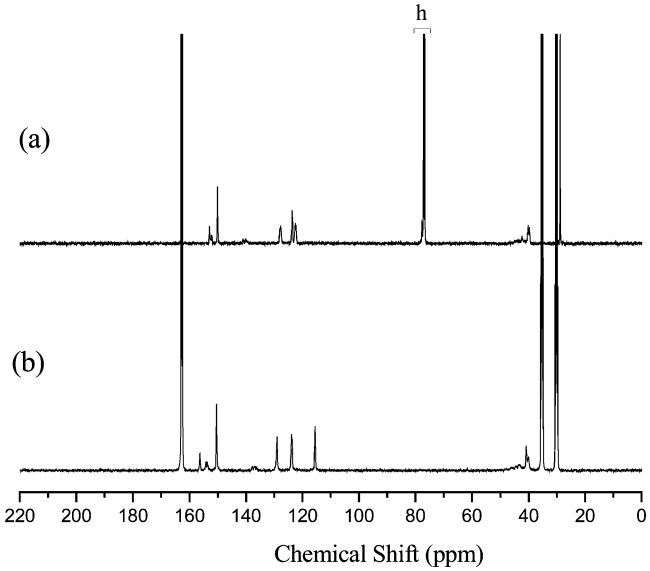

Figure 2. ^{13}C NMR spectra: (a) before hydrolysis, P*t*BOS-*b*-PMMA; (b) after hydrolysis, PVPh-*b*-PMMA.

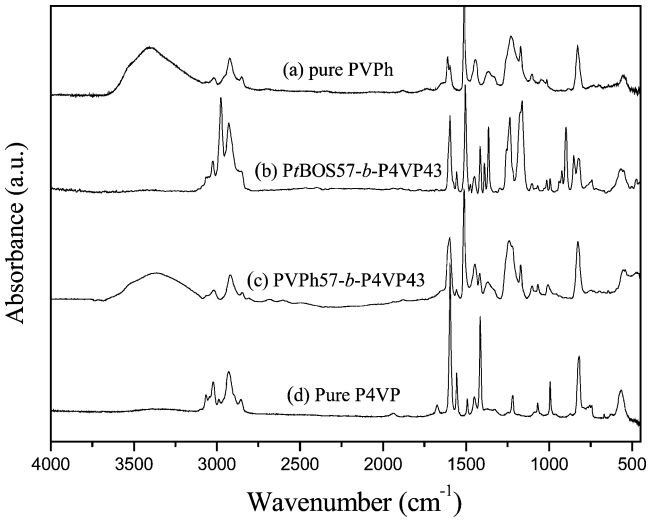

Figure 3. IR spectra of (a) pure PVPh, (b) P*t*BOS-*b*-P4VP, (c) PVPh-*b*-P4VP, and (d) pure P4VP at room temperature ranging from 400 to 4000 cm^{-1}.

−78 °C, the 4-*tert*-butoxystyrene was added, and an aliquot the of poly(4-*tert*-butoxystyrene) sample was isolated for analysis after termination with degassed methanol. A second block was created by slowly adding the 4-vinylpyridine, again maintaining similar reactor temperature. The polymerization was also terminated by degassed methanol. The P*t*BOS-*b*-P4VP diblock copolymer product was dissolved in dioxane/DMF, and then a 10-fold excess of concentrated HCl was added to the solution. The hydrolysis was completed overnight at 100 °C under an argon atmosphere, and then the product was precipitated in cool water. After neutralization with 10 wt % NaOH solution to a pH value of 6−7, the copolymer was filtered off. The resulting polymer underwent two dissolve (DMF)/precipitate (water) cycles and purified by the Soxhlet extraction with water for 72 h before being dried under vacuum at 85 °C. Finally, the poly(vinylphenol-*b*-4-vinylpyridine) (PVPh-*b*-P4VP) diblock copolymer was obtained, and the reaction mechanism is shown in Scheme 1.

Blend Preparations. The PVPh/P4VP complex was prepared by dissolving pure PVPh and pure P4VP separately in methanol. Each solution was stirred overnight to ensure complete dissolution. The two solutions were then mixed together in a molar ratio of 1:1 to give a white precipitate, which was filtered and washed with methanol. The samples were then dried under vacuum to remove

Table 1. Molecular Characterization of Poly(vinylphenol-*b*-4-vinylpyridine) Diblock Copolymers Prepared by Anionic Polymerization

precursor copolymer	copolymer	$M_{n,PtBOS}$[a]	total M_n[a]	PVPh (mol %)[b]	M_w/M_n[a]	T_g (°C)
P*t*BOS	PVPh	20 000	13 600	100	1.05	180
P*t*BOS$_{90}$-*b*-P4VP$_{10}$	PVPh$_{90}$-*b*-P4VP$_{10}$	20 000	22 000	90	1.17	190
P*t*BOS$_{57}$-*b*-P4VP$_{43}$	PVPh$_{57}$-*b*-P4VP$_{43}$	13 600	20 000	57	1.11	207
P*t*BOS$_{50}$-*b*-P4VP$_{50}$	PVPh$_{50}$-*b*-P4VP$_{50}$	8 000	13 000	50	1.15	212
P*t*BOS$_{34}$-*b*-P4VP$_{76}$	PVPh$_{34}$-*b*-P4VP$_{76}$	7 200	21 000	34	1.10	202
P*t*BOS$_{29}$-*b*-P4VP$_{71}$	PVPh$_{29}$-*b*-P4VP$_{71}$	5 900	16 000	29	1.13	199
	P4VP		10 000	0	1.17	150

[a] Polydispersity index and molecular weight, measured by GPC, of the whole diblock copolymer in the form of P*t*BOS-*b*-P4VP. [b] Obtained from ^{1}H NMR measurement.

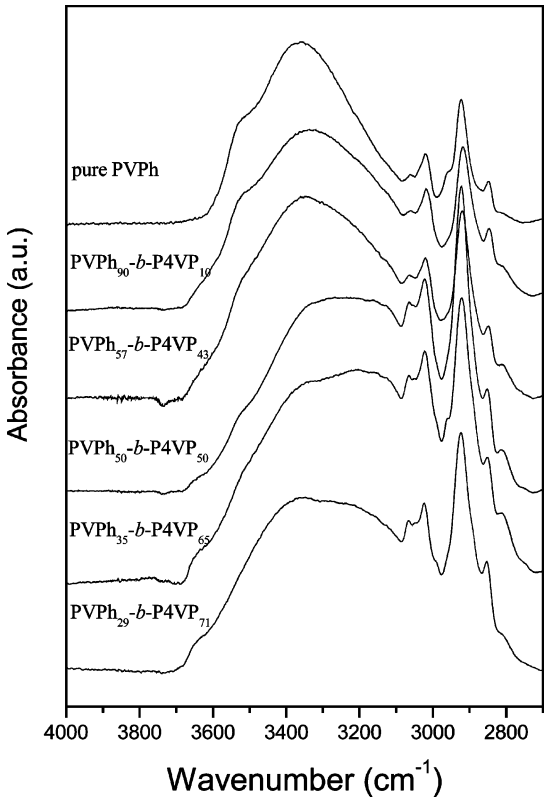

Figure 4. IR spectra, recorded at room temperature, of the hydroxyl region of PVPh-*b*-P4VP diblock copolymers cast from DMF solutions.

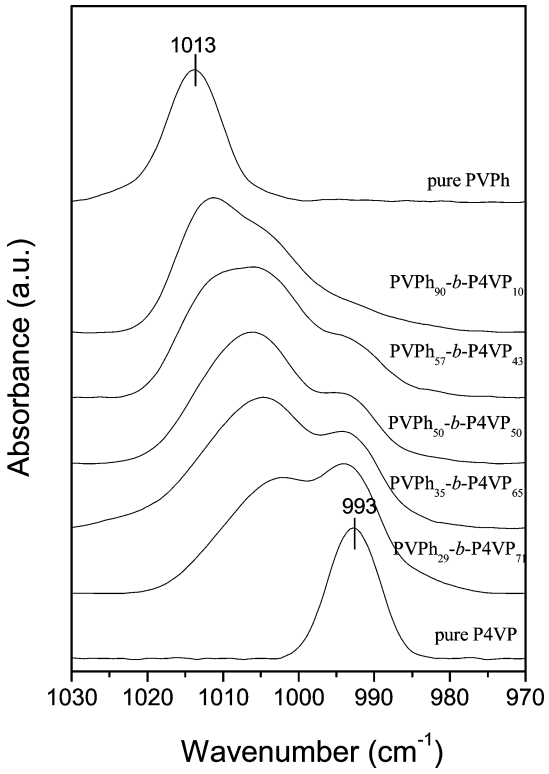

Figure 5. IR spectra, recorded at room temperature, of the region between 1030 and 970 cm^{-1} of PVPh-*b*-P4VP diblock copolymers cast from DMF solutions.

all the residue solvent. The polymer blend between PVPh and P4VP was prepared through solution casting from DMF solution with 5 wt % polymer mixture to avoid complex formation. The mixture was stirred for 6−8 h and then poured into a Teflon dish. The Teflon dish was placed on a hot plate at 80−100 °C to evaporate the solvent slowly for 2 days. The blend film was then dried at 90 °C in vacuum for at least 1 week.

Characterizations. Molecular weight and molecular weight distribution were determined through gel permeation chromatography (GPC) using a Waters 510 HPLC equipped with a 410 differential refractometer, a RI detector, and an UV detector. Three Ultrastyragel columns (100, 500, and 10^3 Å) were connected in series and the THF as eluent at a flow rate of 0.6 mL/min and at 35 °C. The molecular weight calibration curve was obtained using polystyrene standards. ^{1}H NMR and ^{13}C NMR spectra were obtained using an INOVA 500 instrument; chloroform-*d* and *N*,*N*-dimethylformamide-d_7 were used as the solvent. Molecular weights and P*t*BOS/P4VP ratios of various types of copolymers were evaluated from ^{1}H NMR spectra and compared with corresponding values obtained by GPC. Thermal analysis was performed on a DSC instrument from Du-Pont (DSC-9000) at a scan rate of 20 °C/min over a temperature range from 20 to 250 °C under an atmosphere of dry N_2. The sample was quenched to 20 °C from the melt state for the first scan and then rescanned between 20 and 250 °C. The glass transition temperature (T_g) was obtained as the inflection point of the heat capacity jump recorded at a scan rate of 20 °C/min. All infrared spectra were recorded at 25 °C at a resolution of 1 cm^{-1} over 32 scans on a Nicolet AVATAR 320 FTIR spectrometer and degassed with nitrogen. Each sample was dissolved in *N*,*N*-dimethylformamide (DMF) and then cast directly onto a KBr pellet. All films were vacuum-dried and were thin enough to be within the absorbance range where the Beer−Lambert law is obeyed. High-resolution solid-state ^{13}C NMR experiments were carried out at room temperature using a Bruker DSX-400 spectrometer operating at resonance frequencies of 399.53 and 100.47 MHz for ^{1}H and ^{13}C, respectively. The ^{13}C CP/MAS spectra were measured with a 3.9 μs 90° pulse, with 3 s pulse delay time, acquisition time of 30 ms, and 2048 scans. All NMR spectra were taken at 300 K using broadband proton decoupling and a normal cross-polarization pulse sequence. A magic angle sample spinning (MAS) rate of 5.4 kHz was used to avoid absorption overlapping. The proton spin−lattice relaxation time in the rotating frame ($T_{1\rho}$(H)) was determined indirectly via carbon observation using a 90°−τ−spin lock pulse sequence prior to cross-polarization. The data acquisition was performed via ^{1}H decoupling and delay time ranging from 0.1 to 20 ms with a contact time of 1.0 ms.

Results and Discussion

Syntheses of Poly(vinylphenol-*b*-4-vinylpyridine) Diblock Copolymers. The P*t*BOS-b-P4VP diblock copolymer was prepared by sequential anionic polymerization. The poly(4-*tert*-

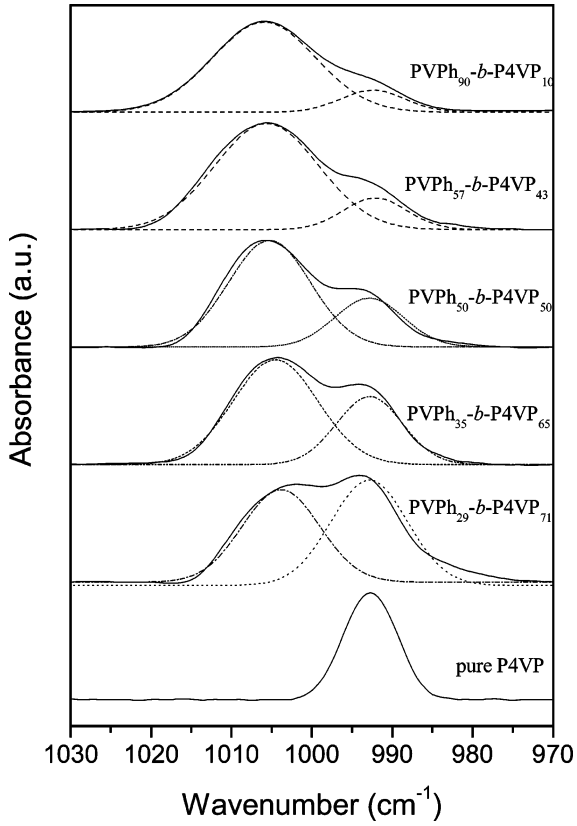

Figure 6. Digital subtracted the pure PVPh peak at 1013 cm^{-1} based on their mole fractions of PVPh in PVPh-*b*-P4VP diblock copolymers.

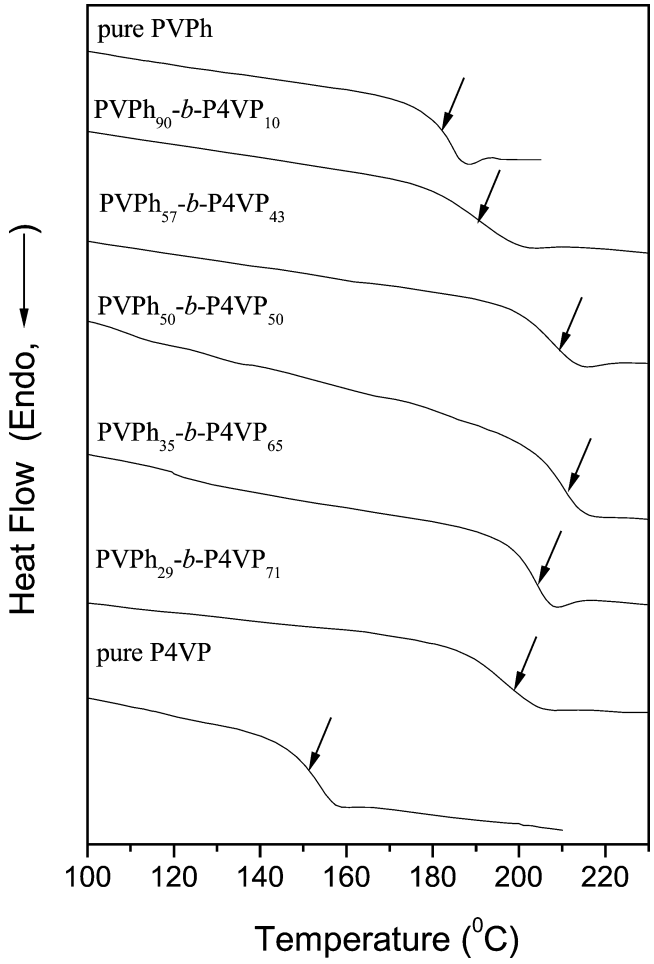

Figure 7. DSC curves of the PVPh-*b*-P4VP diblock copolymers with different PVPh compositions.

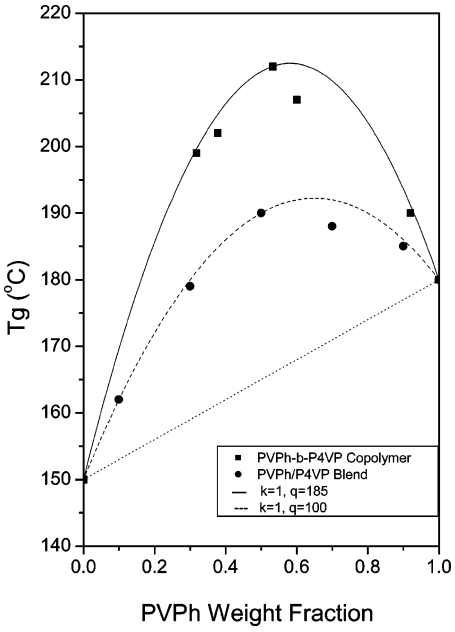

Figure 8. T_g vs composition curves based on Kwei equation for blends and diblock copolymers.

butoxystyrene) block in the block copolymer was hydrolyzed to its acid form, poly(vinylphenol), in dioxane/DMF at 100 °C by refluxing overnight in the presence of concentrated HCl and giving a PVPh-*b*-P4VP diblock copolymer quantitatively (Scheme 1). The molecular weight and the polydispersity of the homo-P*t*BOS and P*t*BOS-*b*-P4VP diblock copolymers were analyzed by gel permeation chromatography (GPC).

The successful synthesis of the diblock copolymer was confirmed on the basis of analysis of ^{1}H MNR spectroscopy. Figure 1 shows the NMR spectrum of the diblock together with assignments of those key peaks. Total elimination of the protective groups and the generation of the phenolic hydroxyl groups were verified by ^{1}H and ^{13}C NMR spectroscopies. Figure 1a,b displays typical ^{1}H NMR spectra of the diblock copolymers recorded before and after deprotection. A chemical shift at 1.29 ppm corresponds to the *tert*-butyl group of the P*t*BOS-*b*-P4VP copolymer (in chloroform-*d*) This characteristic peak (1.29 ppm) corresponding to the *tert*-butyl group is essentially disappeared in the hydrolyzed block copolymer, only those backbone protons appear in the chemical shift region of 1−2 ppm. In addition, a peak (7.9 ppm) corresponding to the proton of the hydroxyl group appears after hydrolysis reaction. The signal of the quarternary carbon atoms of the *tert*-butyl group in the P*t*BOS segment is located at 78.0 ppm[28] (Figure 2a). After the hydrolysis reaction, no signal remains for the *tert*-butyl group, indicating that the hydrolysis reaction was completed. Figure 2b displays the ^{13}C NMR spectra of the PVPh-*b*-P4VP copolymer. The FTIR spectrum (Figure 3) of P*t*BOS-*b*-P4VP shows the pyridine ring absorptions at 980 cm^{-1}, and the resulting block copolymer after hydrolysis (PVPh-*b*-P4VP) clearly shows a broad peak at 3450 cm^{-1}, indicating the presence of the OH group after deprotection. The compositions of the PVPh-*b*-P4VP block copolymers are essential identical as the compositions of the corresponding P*t*BOS-*b*-P4VP. The composition of the P*t*BOS-*b*-P4VP block copolymer was determined from the relative intensities from peaks of the aromatic ring and the pyridine ring in the ^{1}H NMR spectrum. The signals due to the aromatic protons and the pyridine ring were observed at 6.1−6.9 and 8.1−8.2 ppm, respectively.[29] The molecular

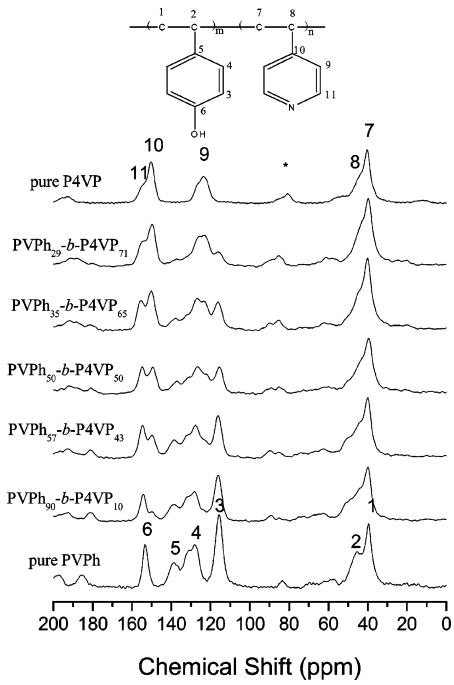

Figure 9. ^{13}C CP/MAS NMR for PVPh-*b*-P4VP diblock copolymers with different PVPh compositions.

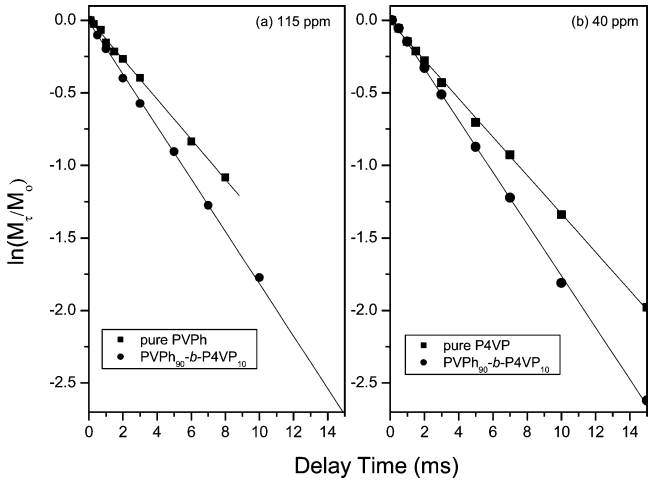

Figure 10. Logarithmic plots of the intensities of (a) 40 and (b) 115 ppm vs delay time.

parameters of the polymers are listed in Table 1. The polymers are denoted as PVPh$_n$-*b*-P4VP$_m$, where *n* and *m* stand for the molecular molar fractions of PVPh and P4VP blocks, respectively. For example, PVPh$_{90}$-*b*-P4VP$_{10}$ represents a diblock copolymer containing 90 mol % of poly(vinylphenol).

FTIR Analyses. FTIR spectroscopy has been successfully applied in numerous diblock copolymers and blends possessing intermolecular interaction through hydrogen bonding. The hydroxyl stretching region in infrared spectrum of the PVPh-*b*-P4VP diblock copolymer is sensitive to hydrogen-bonding interaction. The hydroxyl stretching of pure PVPh and PVPh-*b*-P4VP diblock copolymers cast from DMF solution at room temperature is shown in Figure 4. Pure PVPh shows two unresolved bands in the hydroxyl stretching region, corresponding to the free hydroxyl at 3525 cm^{-1} and a broad band centered at 3350 cm^{-1} from the absorption of hydrogen-bonded hydroxyl group (self-association). Figure 4 also illustrates that the intensity of the free hydroxyl group decreases gradually with the increase

Table 2. Curve Fitting of Fraction of Hydrogen-Bonding Results of PVPh-*b*-P4VP at Room Temperature

	free pyridine ring			H-bonded pyridine ring			
block copolymer	ν, cm^{-1}	$W_{1/2}$	A_f, %	ν, cm^{-1}	$W_{1/2}$	A_b, %	f_b, %
PVPh$_{29}$-*b*-P4VP$_{71}$	993	11	52.9	1004	11	47.1	47.1
PVPh$_{34}$-*b*-P4VP$_{76}$	993	10	33.5	1004	12	66.5	66.5
PVPh$_{50}$-*b*-P4VP$_{50}$	993	10	27.8	1005	12	72.2	72.2
PVPh$_{57}$-*b*-P4VP$_{43}$	993	9	15.5	1005	12	84.5	84.5
PVPh$_{90}$-*b*-P4VP$_{10}$	993	9	13.1	1005	14	86.9	86.9

Table 3. Chemical Shifts (ppm) Observed in the ^{13}C CP/MAS/DD NMR Spectra of PVPh and P4VP Units in Their Block Copolymers

	PVPh				
block copolymer	C-1,2	C-3	C-4	C-5	C-6
pure PVPh	39.7	115.6	128.0	138.5	153.3
PVPh$_{90}$-*b*-P4VP$_{10}$	39.9	115.9	127.9	138.7	153.9
PVPh$_{57}$-*b*-P4VP$_{43}$	40.0	115.9	127.4	138.3	154.3
PVPh$_{50}$-*b*-P4VP$_{50}$	40.4	116.2	127.4	137.8	155.4
PVPh$_{34}$-*b*-P4VP$_{76}$	40.1	115.9	126.6	137.5	155.0
PVPh$_{29}$-*b*-P4VP$_{71}$	40.7	116.8	126.3	137.9	154.5

	P4VP			
block copolymer	C-7,8	C-9	C-10	C-11
PVPh$_{90}$-*b*-P4VP$_{10}$	39.9	124.0	149.6	153.9
PVPh$_{57}$-*b*-P4VP$_{43}$	40.0	122.8	149.6	154.3
PVPh$_{50}$-*b*-P4VP$_{50}$	40.4	122.7	150.2	155.4
PVPh$_{34}$-*b*-P4VP$_{76}$	40.1	123.1	149.9	155.0
PVPh$_{29}$-*b*-P4VP$_{71}$	40.7	123.9	150.5	154.5
pure P4VP	40.7	123.5	150.2	154.5

of the P4VP content in diblock copolymer as would be expected. This free hydroxyl peak is essentially disappeared when the P4VP content in the diblock copolymer reaches 74 mol %, indicating that more free hydroxyl groups are hydrogen bonded with pyridine groups as the concentration of pyridine groups is increased. Meanwhile, the peak frequency of the broad band shifts to lower wavenumber with increasing P4VP content, reflecting that a new distribution of hydrogen-bonding formation resulting from the competition between the hydroxyl−hydroxyl group within the pure PVPh and the hydroxyl−pyridine group between PVPh and P4VP. It also reveals that interaction between PVPh hydroxyl and P4VP pyridine becomes dominant in those P4VP-rich diblock copolymers. Therefore, it is reasonable to assign the bands at 3125 cm^{-1} as the hydrogen-bonding interactions between PVPh hydroxyl and P4VP pyridine block. Coleman and co-workers have used the frequency difference between the hydrogen-bonded hydroxyl absorption and the free hydroxyl absorption ($\Delta\upsilon$) to roughly estimate the average hydrogen-bonding strength.[30] In this respect, hydrogen-bonding interactions between PVPh hydroxyl and P4VP pyridine in diblock copolymer ($\Delta\upsilon = 400$ cm^{-1}) are stronger than that of the pure PVPh ($\Delta\upsilon = 175$ cm^{-1}).

Besides the hydroxyl stretching region, some characteristic modes of the pyridine ring are sensitive to hydrogen-bonding interaction. These modes including 1590, 1050, 993, and 625 cm^{-1} shift to 1600, 1067, 1011, and 634 cm^{-1} after forming hydrogen-bonding interaction with the carboxylic acid groups of poly(ethylene-*co*-methacrylic acid).[31] Unfortunately, the bands at 1590 cm^{-1} for P4VP are difficult to analyze due to overlapping with the 1600 cm^{-1} band from the PVPh. Therefore, only the band at 993 cm^{-1} can be used to analyze the hydrogen-bonding interactions between the hydroxyl group of PVPh and the pyridine group of P4VP. Figure 5 shows the scale-expanded infrared spectra in the range 970−1030 cm^{-1} measured at room temperature for pure PVPh, P4VP, and PVPh-*b*-P4VP diblock copolymers. Pure P4VP has a characteristic band at 993 cm^{-1}, corresponding to the pure pyridine ring absorption. Pure PVPh

Table 4. Relaxation Times, $T_{1\rho}^{H}$, for Blends, Blend Complex, and Diblock Copolymers at the Magnetization Intensities of 40 and 115 ppm

40 ppm				115 ppm			
PVPh/P4VP[a]	$T_{1\rho}^{H}$ (ms)	PVPh-*b*-P4VP	$T_{1\rho}^{H}$ (ms)	PVPh/P4VP[a]	$T_{1\rho}^{H}$ (ms)	PVPh-*b*-P4VP	$T_{1\rho}^{H}$ (ms)
				100/0	8.79		8.79
30/70	7.80	28-*b*-72	6.55	30/70	10.70	28-*b*-72	7.07
50/50	8.40	50-*b*-50	6.92	50/50	9.40	50-*b*-50	7.09
70/30	8.69	90-*b*-10	5.60	70/30	9.10	90-*b*-10	5.53
complex	7.26			complex	7.11		
0/100	7.56	0/100	7.56				

[a] Reference 9.

does not absorb at 993 cm^{-1} but has a band at 1013 cm^{-1}. These two bands are well resolved without overlapping. Upon copolymerization the PVPh with P4VP, a new appeared band at 1005 cm^{-1} is assigned to hydrogen-bonded pyridine rings, corresponding to the P4VP block of the PVPh-*b*-P4VP copolymer. All IR spectra show the existence of hydrogen bonding between pyridine group and hydroxyl group from all copolymers. It is difficult to calculate the quantitative fraction of hydrogen bonding due to the presence of three bands in this region. As a result, the digital subtraction of the pure PVPh peak at 1013 cm^{-1} based on its mole fraction of the PVPh in these diblock copolymers was carried out as shown in Figure 6. Clearly, only two bands are found in Figure 6: a characteristic band at 993 cm^{-1} corresponding to the pure pyridine ring absorption and a new band from the hydrogen-bonded pyridine ring at 1005 cm^{-1}. All these pyridine frequencies split into two bands that can be fitted well to the Gaussian function as also shown in Figure 6. The fraction of the hydrogen-bonded pyridine ring can be calculated by the following equation:[2]

$$f_b = \frac{A_b/a}{A_b/a + A_f} \tag{1}$$

A_f and A_b are peak areas corresponding to absorptions from the free and the hydrogen-bonded pyridine ring, respectively. The conversion coefficient (a) is the specific absorption ratio of these two bands, free and hydrogen-bonded pyridine ring. The conversion coefficient (a) = 1 from a similar system has been determined previously.[32] Results from curve fitting are summarized in Table 2; the hydrogen-bonded fraction of the pyridine ring increases with the increase of the PVPh content in these diblock copolymers, which is similar to our previously reported phenolic/P4VP blends.[33]

Thermal Analyses. Generally, it is believed that only a single glass transition temperature can be observed if components of blends and block polymers are thermodynamically miscible. Differential scanning calorimetry (DSC) is a convenient method for observing the thermal characteristics that arise from the different interactions of miscible block copolymers and polymer blends. Figure 7 presents the DSC thermograms of various PVPh-*b*-P4VP block copolymers containing different PVPh contents, indicating that all PVPh-*b*-P4VP copolymers have only a single glass transition temperature. This finding suggests strongly that these diblock copolymers are fully miscible with homogeneous amorphous phase. Meanwhile, a single T_g higher than that of either individual polymer was observed. The large positive T_g deviation indicates that the strong interaction exists between these two block components. This result is similar to the T_g behavior of PVPh/P4VP miscible blend system from DMF solution (see Figure 8). Figure 8 shows the T_g composition curves for the diblock copolymers and corresponding miscible blends. For miscible blends and diblock copolymers, T_g can be described by several empirical equations,[34−36] and the Kwei equation[36] is usually employed for systems with specific interactions

$$T_g = \frac{W_1 T_{g1} + kW_2 T_{g2}}{W_1 + kW_2} + qW_1 W_2 \tag{2}$$

where w_1 and w_2 are weight fractions of the compositions, T_{g1} and T_{g2} represent the corresponding glass transition temperatures, and k and q are fitting constants. Figure 8 shows the dependence of the T_g on the composition of the miscible diblock copolymer and blend of PVPh/P4VP, where the maximum deviation on the highest T_g is obtained when block copolymer and blend composition are at ca. PVPh/P4VP = 50/50. In this study, k = 1 and q = 185 for the diblock copolymers and k = 1 and q = 100 for the blends were obtained from the nonlinear least-squares "best fit" approach as shown in Figure 8. Here q is a parameter corresponding to the strength of hydrogen bonding in the system, reflecting a balance between the breaking of the self-association and the forming of the interassociation hydrogen bonding. These positive q values of 185 and 100 obtained indicate that interassociation hydrogen-bonding interaction existed between the hydroxyl group of PVPh and the pyridine group of P4VP in copolymers is stronger than corresponding blend, which is similar to our previous studies.[19,22] Here, we ignore the effect of stereotactic configuration and molecular weight on the formation of intermolecular hydrogen bonds in T_g behavior.

More importantly, the PVPh-*b*-P4VP diblock copolymer shows a single T_g at 212 °C at a 1:1 (PVPh:P4VP) molar ratio, which is closed to the value of PVPh/P4VP = 1:1 complex (210 °C) from methanol solution as mentioned previously. Jiang et al.[37,38] have reported that a ordinary miscible blend is able to form an interpolymer complex by increasing the density of intermolecular hydrogen bonds, and the transition from separated polymer coils to complex aggregates takes place in solution as the intermolecular hydrogen bonding is strong. Moreover, they found that, in the solid state, further strengthening of hydrogen bonding can transform a miscible blend into the complex state. In our case, the T_g behavior difference between the PVPh/P4VP miscible blend and the PVPh-*b*-P4VP diblock copolymer may follow the similar trend. As a result, we may conclude that the polymer chain behavior in diblock copolymer is similar to that of the interpolymer complex. In order to confirm this conclusion, we will explore the homogeneity and phase behavior of polymer blend and diblock copolymer by spin−lattice relaxation time in the rotating frame using solid-state NMR in the next section.

Solid-State NMR Analyses. In addition to FT-IR, evidence on interactions in the diblock copolymers and the blends can also be obtained from solid-state NMR spectroscopy as demonstrated by changes in chemical shift and/or line shape. Figure 9 shows the selected ^{13}C CP/MAS spectra of various PVPh-*b*-P4VP copolymers. The pure PVPh displays five peaks where the phenolic atom (C-6) is at δ = 153.3 ppm. Five peaks are

Scheme 2. Physical Picture of Polymer Chain for Miscible Blend and Miscible Diblock Copolymer

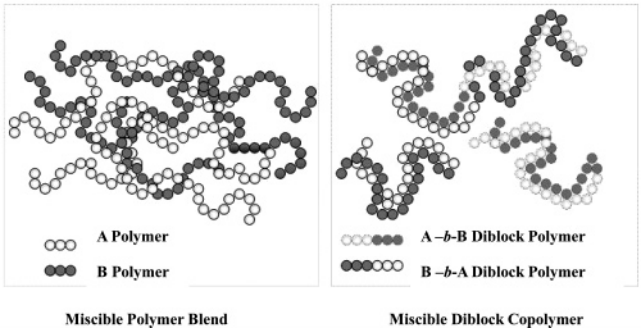

also observed for pure P4VP where the peak at $\delta = 154.5$ ppm corresponds to the pyridine carbon atom (C-11). All other peaks are also assigned in Figure 9. Table 3 summarizes the values of the chemical shifts observed in the ^{13}C CP/MAS NMR spectra of PVPh-*b*-P4VP copolymers. Since most peaks between these two polymers are overlapped, it is difficult to characterize the interaction between their functional groups. However, for the $PVPh_{50}$-*b*-$P4VP_{50}$ diblock copolymer, the phenolic and pyridine carbons shift downfield to 155.4 ppm significantly (both larger than 153.3 and 154.5 ppm), also indicating the hydrogen-bonding interaction between the hydroxyl group of PVPh and the pyridine group of P4VP.

Solid-state NMR spectroscopy has also been used to better understand the phase behavior and miscibility of diblock copolymers and blends. A single T_g based on DSC analysis implies that the mixing of two blending components is in a scale of about 20−40 nm.[4] The dimension of mixing smaller than 20 nm can be obtained through measurement of the spin−lattice relaxation time in the rotating frame ($T_{1\rho}^H$).[4] The $T_{1\rho}^H$ values of the diblock copolymers and blend complex were measured through the delayed-contact ^{13}C CP/MAS experiments. The $T_{1\rho}^H$ values were calculated from eq 3:

$$M_\tau = M_0 \exp[-\tau/T_{1\rho}^H] \quad (3)$$

where τ is the delay time used in the experiment and M_τ is the corresponding resonance intensity. Figure 10 shows plots of ln-(M_τ/M_0) vs τ for the P4VP resonance (40 ppm, (a)) and the PVPh resonance (115 ppm, (b)) of the diblock copolymers. The experimental data are in good agreement with eq 3. From the slope of the fitting line, the $T_{1\rho}^H$ value can be determined. Table 4 lists the results of the $T_{1\rho}^H$ values for diblock copolymers, blends, and blend complex. A single composition-dependent $T_{1\rho}^H$ was obtained for all diblock copolymers, blends, and blend complex, suggesting that they are homogeneous to a scale where the spin diffusion occurs within the time $T_{1\rho}^H$. The upper spatial scale of the spin-diffusion path length L can be estimated from the following expression:[39]

$$L = (6DT)^{1/2} \quad (4)$$

where D, typically at 10^{-16} m^2 s^{-1}, is the effective spin-diffusion coefficient depending on the average proton to proton distance as well as the dipolar interaction (Table 4). Therefore, the upper limit of the domain size for blends is estimated to be 2 nm while that of the diblock copolymers and blend complex are estimated to be 1.5 nm. In addition, $T_{1\rho}^H$ values for blends are higher than those two pure polymers, but $T_{1\rho}^H$ values of diblock copolymers and blend complex are lower than those of two pure polymers. In addition, the $T_{1\rho}^H$ value for diblock copolymer is

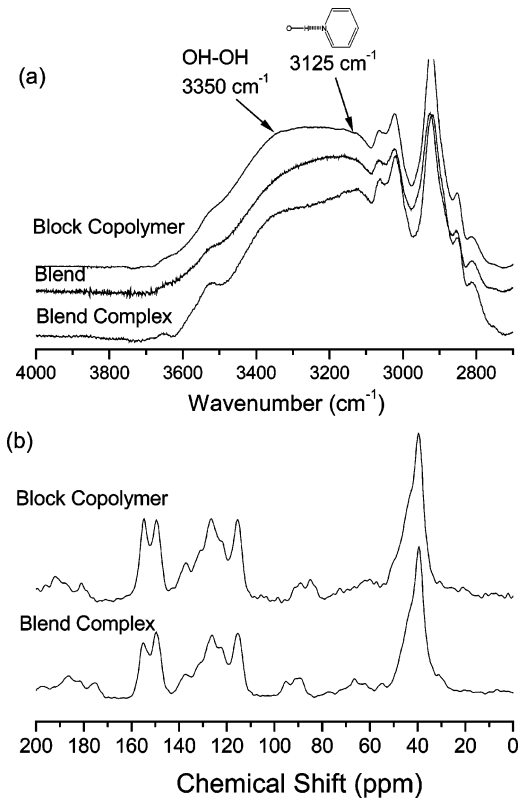

Figure 11. FTIR spectra (a) and ^{13}C solid-state NMR (b) of diblock copolymer, blend complex, and blend at PVPh:P4VP = 1:1 ratio.

slightly lower than the blend complex, which is consistent with our DSC analyses that the T_g for diblock copolymer is higher than blend complex ca. 2 °C (212 °C:210 °C). All results imply that diblock copolymers have relatively smaller domain sizes than the corresponding blends, indicating that the degrees of homogeneity of diblock copolymers are relatively higher than those of the blends. As a result, the shorter $T_{1\rho}^H$ relaxation time of the block copolymer means more rigid nature of the polymer chain and enhances its T_g. By comparing polymer blend of poly-(acrylic acid) (PAA)/poly(vinylpyrrolidone) (PVP) with complex of PAA/PVP, resultant $T_{1\rho}^H$ values show the same trend that the complex of PAA/PVP is shorter than the corresponding blend.[40] Figure 11 shows the infrared spectra at hydroxyl stretching (a) and ^{13}C solid-state NMR (b) analyses of diblock copolymer, blend complex, and blend at PVPh:P4VP = 1:1 ratio. Clearly, we can find that the chemical shifts of phenolic atom (C-6) at $\delta = 153.3$ ppm for both diblock copolymer and blend complex shift downfield to the same amount (155.4 ppm). In addition, the infrared spectra of the hydroxyl frequency for the hydroxyl−pyridine is also shifted to the same amount (at 3125 cm^{-1}) in the blend as in the block copolymer and blend complex, suggesting that the strength of the hydrogen bond in all systems is identical. However, the relative intensity ratio of the hydroxyl−hydroxyl relative to the hydroxyl−pyridine hydrogen-bonded peak in diblock copolymer is the largest, indicating that the intrachain contacts are playing an important role. As a result, the T_g behavior difference between blend and diblock copolymer may come from the different chain behavior. On the basis of DSC, solid-state NMR, and FTIR analyses, we can conclude that the polymer chain behavior for strong hydrogen-bonded PVPh-*b*-P4VP diblock copolymer is in the form of complex aggregates, similar to the interpolymer complex of PVPh/P4VP obtained from methanol solution. More interestingly, the polymer blend complex in low polar solvent occurs only on the blend with PVPh/P4VP = 1:1 molar ratio. However, the

complex aggregates from diblock copolymer can be easy controlled their T_g by changing the mole fraction of PVPh through anionic polymerization synthesis method. Scheme 2 summarizes the physical picture of polymer chains for miscible polymer blend and miscible diblock copolymer. Polymer coils are well separated for a miscible polymer blend in a strong polar solvent (such as DMF solution). All polymer chains are rather extended before solvent evaporation because the interassociation hydrogen bonding between PVPh/DMF is stronger than PVPh/P4VP blend.[38] However, the higher intrachain hydrogen bonding in diblock copolymer chain tends to induce polymer complex aggregation. Two possible mechanisms may involve the formation of the interpolymer complex through two individual diblock copolymer chains by interchain hydrogen-bonding interaction and the formation of the intrapolymer complex through folding the same diblock copolymer chain by intrachain hydrogen-bonding interaction. For a polymer blend complex, the interpolymer complex is only existed via individual polymer chain, which is consistent with the infrared analysis that the relative intensity ratio of the hydroxyl−hydroxyl relative to the hydroxyl−pyridine hydrogen-bonded peak in blend complex is the lowest, indicating that most interactions are from the interchain contacts. As a result, both inter- and intrapolymer complexes in diblock copolymer have the smaller domain size than the relatively more separated coils in miscible blend, which is consistent with our $T_{1\rho}^{H}$ values.

Conclusions

We have successfully synthesized diblock copolymers of PVPh with P4VP through anionic polymerization. From DSC analyses, we observed higher glass transition temperatures for PVPh-*b*-P4VP copolymers relative to their corresponding PVPh/P4VP blends as a result of stronger intrachain hydrogen bonding existing in the former copolymer system. FTIR and solid-state NMR spectroscopic analyses provided evidence that the specific interaction in the PVPh-*b*-P4VP copolymer arises from the hydroxyl group of PVPh and the pyridine group of PVP, similar to that observed for the PVPh/P4VP blend system. The higher values of T_g for the PVPh-*b*-P4VP copolymers relative to those for the PVPh/P4VP blends are probably caused by the inter- and intrapolymer complex aggregates occurring in the diblock copolymer, which is similar to the PVPh/P4VP complex obtained in methanol solution. Measurements of $T_{1\rho}^{H}$ reveal that the calculated domain sizes of the diblock copolymers are relatively smaller than the corresponding blends. This result is able to provide positive evidence that polymer complex aggregate in diblock copolymer have the smaller domain size due to the shorter $T_{1\rho}^{H}$ value than the separated coils in the miscible blend.

Acknowledgment. This research was supported financially by the National Science Council, Taiwan, Republic of China, under Contract NSC-95-2216-E-009-001 and Ministry of Education "Aim for the Top University" program (MOEATU program).

References and Notes

(1) Utracki, L. A. *Polymer Alloys and Blends: Thermodynamics and Rheology*; Carl Hanser Verlag: Munich, 1989.

(2) Coleman, M. M.; Graf, J. F.; Painter, P. C. *Specific Interactions and the Miscibility of Polymer Blends*; Technomic Publishing: Lancaster, PA, 1991.

(3) Coleman, M. M.; Painter, P. C. *Prog. Polym. Sci.* **1995**, *20*, 1.

(4) Kuo, S. W.; Chang, F. C. *Macromolecules* **2001**, *34*, 4089.

(5) Kuo, S. W.; Chang, F. C. *Macromolecules* **2001**, *34*, 5224.

(6) He, Y.; Zhu, B.; Inoue, Y. *Prog. Polym. Sci.* **2004**, *29*, 1021.

(7) de Mefathi, M. V.; Frechet, J. M. J. *Polymer* **1988**, *29*, 477.

(8) Dai, J.; Goh, S. H.; Lee, S. Y.; Siow, K. S. *Polym. J.* **1994**, *26*, 905.

(9) Wang, J.; Cheung, M. K.; Mi, Y. *Polymer* **2001**, *42*, 3087.

(10) Xiang, M.; Jiang, M.; Zhang, Y.; Wu, C. *Macromolecules* **1997**, *30*, 2313.

(11) Zhang, Y.; Xiang, M.; Jiang, M.; Wu, C. *Macromolecules* **1997**, *30*, 6084.

(12) Serman, C. J.; Painter, P. C.; Coleman, M. M. *Polymer* **1991**, *32*, 1049.

(13) Zhang, X.; Takegoshi, K.; Hikichi, K. *Macromolecules* **1991**, *24*, 5756.

(14) Li, D.; Brisson, J. *Macromolecules* **1996**, *29*, 868.

(15) Dong, J.; Ozaki, Y. *Macromolecules* **1997**, *30*, 286.

(16) Kuo, S. W.; Liu, W. P.; Chang, F. C. *Macromolecules* **2003**, *36*, 5165.

(17) Kuo, S. W.; Liu, W. P.; Chang, F. C. *Macromol. Chem. Phys.* **2005**, *206*, 2307.

(18) Wang, L. F.; Pearce, E. M.; Kwei, T. K. *J. Polym. Sci., Polym. Phys. Ed.* **1991**, *29*, 619.

(19) Lin, C. L.; Chen, W. C.; Liao, C. S.; Su, Y. C.; Huang, C. F.; Kuo, S. W.; Chang, F. C. *Macromolecules* **2005**, *38*, 6435.

(20) Painter, P. C.; Coleman, M. M. *Polymer Blends*; Paul, D. R., Ed.; John Wiley & Sons: New York, 2000; Vol. 1.

(21) Coleman, M. M.; Xu, Y.; Painter, P. C. *Macromolecules* **1994**, *27*, 127.

(22) Kuo, S. W.; Huang, C. F.; Tung, P. H.; Huang, W. J.; Huang, J. M.; Chang, F. C. *Polymer* **2005**, *46*, 9348.

(23) Varshney, S. K.; Zhong, X. F.; Eisenberg, A. *Macromolecules* **1993**, *26*, 701.

(24) Quirk, R. P.; Corona-Galvan, S. *Macromolecules* **2001**, *34*, 1192.

(25) Biggs, S.; Vincent, B. *Colloid Polym. Sci.* **1992**, *270*, 505.

(26) Hubert, P.; Soum, A.; Fontanille, M. *Macromol. Chem. Phys.* **1995**, *196*, 1023.

(27) Quirk, R. P.; Lee, Y. *J. Polym. Sci., Part A: Polym. Chem.* **2000**, *38*, 145.

(28) Jiang, X.; Tanaka, K.; Takahara, A.; Kajiyama, T. *Polymer* **1998**, *39*, 2615.

(29) Agata, Y.; Masuda, J.; Noro, A.; Cho, D.; Takano, A.; Matsushita, Y. *Macromolecules* **2005**, *38*, 10220.

(30) Moskala, E. J.; Varnell, D. F.; Coleman, M. M. *Polymer* **1985**, *26*, 228.

(31) Lee, Y. J.; Painter, P. C.; Coleman, M. M. *Macromolecules* **1988**, *21*, 954.

(32) Cesteros, L. C.; Meaurio, E.; Katime, I. *Macromolecules* **1993**, *26*, 2323.

(33) Kuo, S. W.; Lin, C. L.; Chang, F. C. *Polymer* **2002**, *43*, 3943.

(34) Fox, T. G. *J. Appl. Bull. Am. Phys. Soc.* **1956**, *1*, 123.

(35) Gordon, M.; Taylor, J. S. *J. Appl. Chem.* **1952**, *2*, 493.

(36) Kwei, T. K. *J. Polym. Sci., Polym. Lett. Ed.* **1984**, *22*, 307.

(37) Jiang, M.; Li, M.; Xiang, M.; Zhou, H. *Adv. Polym. Sci.* **1999**, *146*, 121.

(38) Ning, F. L.; Jiang, M.; Ning, F. L.; Chen, D. Y.; Liu, S. Y.; Duan, H. W. *Macromolecules* **2002**, *35*, 5980.

(39) McBrierty, V. J.; Douglass, D. C. *J. Polym. Sci., Macromol. Rev.* **1981**, *16*, 295.

(40) Lau, C.; Mi, Y. *Polymer* **2002**, *43*, 823.

MA061713Q